R&D NOTE

Proper Orthogonal Decomposition for the Study of Hydrodynamics in a Mixing Tank

J. Moreau
Institut de Mécanique des Fluides de Toulouse, 31500 Toulouse, France

A. Liné
Laboratoire d'Ingénierie des Procédés de l'Environnement, Institut National des Sciences Appliquées de Toulouse, 31077 Toulouse, Cedex, France

DOI 10.1002/aic.10854
Published online April 26, 2006 in Wiley InterScience (www.interscience.wiley.com).

Keywords: Rushton turbine, turbulence, POD, PIV, mixing, large scale structures

Introduction

The complex flow generated by a Rushton turbine is characterized both by a high-level of turbulence, and by a large-scale structure induced by the blade motion. These coherent structures are a counter-rotating vortex pair (Van'Riet and Smith,[1] Van'Riet et al.,[2] Escudié et al.[3]). They are of critical importance in a mixing tanks, since they are linked with blending performance, gas cavities (in the case of an aereted tank) and turbulence production. It is assumed that the impact of these coherent trailing vorticies in flow-energy transfer is important, and it seems necessary to get a good evaluation of the part of the mean energy transfered to periodic motion, as well as from organized motion to turbulence. However, in an attempt to evaluate these transfers, several techniques have been used in the past. For example, a velocity correlation function can be used to isolate a periodic component associated with a random one with Doppler Velocimetry (Wu and Patterson[4]). However, this kind of technique requires time resolved measurements and cannot be applied in the case of low-speed particle image velocimetry (PIV). Furthermore, in this study we are interested in the spatial properties of the flow induced by the blade, thus, justifying the use of PIV. The other technique is based on the synchronization of the data acquisition with the blade position. It is then possible to separate periodic and turbulent fluctuations (Yiannekis and Whitelaw,[5] Stoots and Calabrese,[6] Schäfer et al.,[7] 2000; Sharp and Adrian,[8] Escudié and Liné[9]). This technique enables the organized motion velocity to be extracted for a given blade position. Escudié and Liné[9] have highlighted that a large amount of energy is transfered between periodic motion and turbulence, thus, explaining the decrease of organized motion energy associated with the increase of turbulent kinetic energy in the jet of a Rushton turbine. PIV investigations to collect the velocity data to compute all of these terms are constraining. First, PIV measurements must be synchronized with the angular position of the impeller in order to perform instantaneous velocity fields for each blade position. It has been shown that a large amount of mean energy is transfered to organized motion in the vicinity of the blades. These transfers can be estimated with measurements of the six components of the tensors of turbulent and organized stresses. Thus, PIV measurements must be performed in different horizontal and vertical planes in a cubic box close to the impeller. The amount of data to be acquired and processed is large. The synchronization of data acquisition with blade positions multiply then by 60 the amount of data. We propose in this work, to use proper orthogonal decomposition (POD) as a complementary analysis tool to study the energy transfer involving the organized motion. It will be shown that this tool allows for the separation of the different motions without the necessity to collect angular phased datas.

First, the experimental database is presented in the next section. The POD principle is described in the Principle of Proper Orthogonal Decomposition section. Then, a large part of the article is dedicated to describing the results, and finally the authors conclude on the efficiency and advantages of such an approach in this context.

Experimental Setup and Velocity Database

The experimental setup consists of a standard cylindrical tank equipped with a Rushton turbine (Figure 1). The cylinder

Correspondence concerning this article should be addressed to A. Liné at line@insa-toulouse.fr.

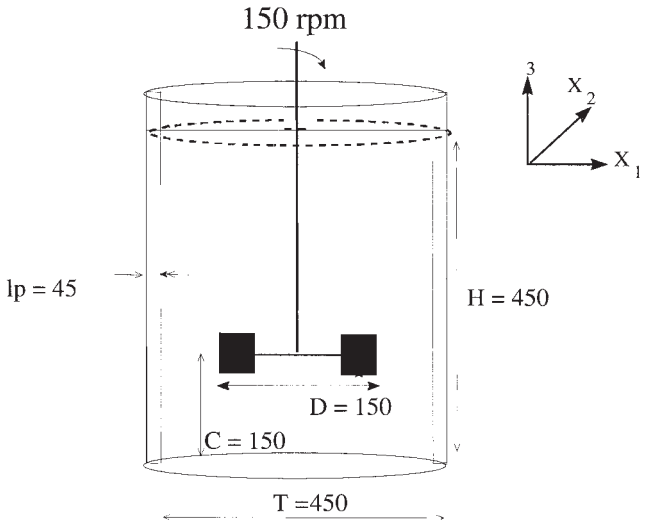

Figure 1. Tank geometry.

is made of glass (6 mm thick) and has a dia. $T = 450$ mm. The liquid (tap water) height is $H = T = 450$ mm, and the flat-bottom tank is open at the top. The tank is equipped with four equally spaced baffles (width $B = T/10 = 45$ mm). Experiments were carried out with a constant impeller speed of 150 rpm. The Reynolds number is $Re = 56250$ ($Re = ND^2/\nu$), the flow is fully turbulent.

The PIV system used was the commercial system acquired from Dantec Measurement Technology. The beam of a double pulsed Nd:Yag Laser (15 hz, 30 mJ) was focused through several optical components to produce a double light sheet in the tank. The double-image recorder camera was a Kodac Megaplus ES 1.0 (1008 × 1018 pixels), for more details concerning PIV setup see Escudié and Liné[9]. Two kinds of data acquisition have been carried out. First, a synchronization of the data acquisition with the blade position is done. In the following, these data will be called "conditioned" data. Second, a nonsynchronized acquisition has been processed, thus, leading to "nonconditioned" data. When phase averaging velocity fields from a given blade position you obtain (Reynolds and Hussain[10])

$$\langle U \rangle = \bar{U} + \tilde{u} \tag{1}$$

The term $\bar{U}$ is obtained, while averaging the all set of "nonconditioned" data. The measurement area is limited to the region close to the impeller. In a previous study (Escudié et al.[3]), measurements in three different planes have been performed in order to calculate the velocity gradient tensor. In this study, we decided to use only vertical-radial plane measurements. The acquisitions are synchronized with the blade positions, and the measurements plane is acquired every 1° blade angle interval.

Principle of Proper Orthogonal Decomposition

POD is a linear procedure, which decomposes a set of signals into a modal base (Lumley[11]). The POD analysis is introduced in this context by the use of physical functions with finite kinetic energy equivalent to the square integrable function. The coherent structures should be the structures that have the largest mean square projection on the velocity field, and are the solutions of the following eigenvalue problem

$$\int\int_D R_{ij}(x, x') \cdot \mathbf{\Phi}_j^{(n)}(x')dx' = \lambda^{(n)}\mathbf{\Phi}_i^{(n)}(x) \tag{2}$$

Sirovich[12] proposed an equivalent approach by using the fact that the two point correlation tensor R_{ij} represents a degenerate kernel so that we can express the eigenfunctions like an admixture of the instantaneous velocity fields

$$\mathbf{\Phi}_i = \sum_{k=1}^{M} b_k^i U_k \tag{3}$$

Where b_k^i are the eigenvectors of the matrix

$$C_{ij} = \frac{1}{M}\sum_{m=1}^{n} U_{(i)}(x_m) \cdot U_{(j)}(x_m) \tag{4}$$

λ^i represents the associated eigenvalues. M is the number of data (velocity fields here) used for the decomposition, n is the number of vectors of the velocity field. The size of the matrix C_{ij} is M by M so that the number of eigenfunctions is M. Actually, $\Sigma_{m=1}^{n} U^{(i)}(x_m) \cdot U^{(j)}(x_m)$ is the inner product between fields $U^{(i)}$ and $U^{(j)}$.

By construction, eigenfunction $\mathbf{\Phi}_i$ has the same size than velocity fields (Eq. 3), but it is important to note that it is not a velocity field but a mathematical basis.

It is important to recall some properties. First the eigenfunctions are normalized and orthogonal, if (,) represents the inner product defined on Eq. 4, then

$$(\mathbf{\Phi}_i, \mathbf{\Phi}_j) = \delta_{ij} \tag{5}$$

If we call a_k^i the result of the projection of the i^{th} mode on the k^{th} instantaneous field, then

$$U_k = \sum_{i=1}^{M} a_k^i \mathbf{\Phi}_i \tag{6}$$

An important property of POD decomposition is that the coefficients a_k^i are uncorrelated with

$$\overline{(a_k^i a_m^i)} = \lambda_k \delta_{km} \tag{7}$$

This property underlines that each mode have a specific contribution to mean field energy independently.

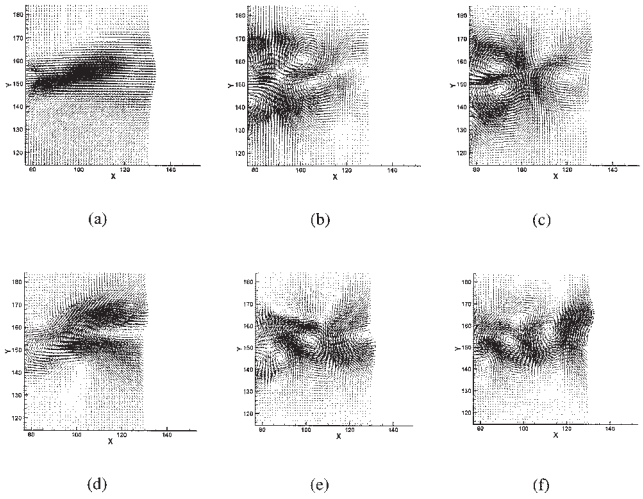

Figure 2. (a) Mode 0, (b) mode 1, (c) mode 2, (d) mode 3, (e) mode 4, (f) mode 5, from POD of the all set of instantaneous velocity fields.

Applications of POD

POD applied to instantaneous velocity fields randomly acquired

First, the POD is carried out using the snapshot method with the complete set of "nonconditioned" instantaneous velocity fields. The result is then an orthonormal basis of eigenfunctions $\{\mathbf{\Phi}_i\}$, and the associated eigenvalues λ_i.

It is shown in Figure 2 that mode 0 is structurally close to the average velocity field (Escudié and Liné[9]). This is a classical result when the POD is carried out with the instantaneous velocity fields. The two following modes reveal large-scale rotating structures. The length scale of these later structures is quite similar to periodic vortex size. It is possible to note in Figure 3 the discontinuity in the eigenvalue scattering. Indeed, the second and third eigenvalues are equal, thus, meaning that the energy of the flow represented by these modes is the same. It can be shown that the energy carried by the three first modes is about 65% of the total energy.

We propose to project instantaneous velocity fields on each POD mode. This projection value gives a good evaluation of the square root of the energy of the instantaneous flow carried by the corresponding mode. Then statistics can be done on the projection value (Patte-Rouland et al.[13]) for a given mode between all the set of instantaneous velocity fields.

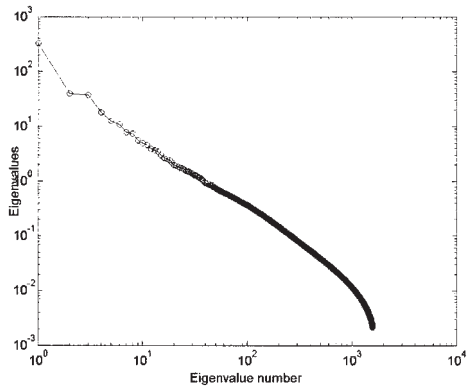

Figure 3. Evolution of the normalized eigenvalue according to the normalized eigenfunction.

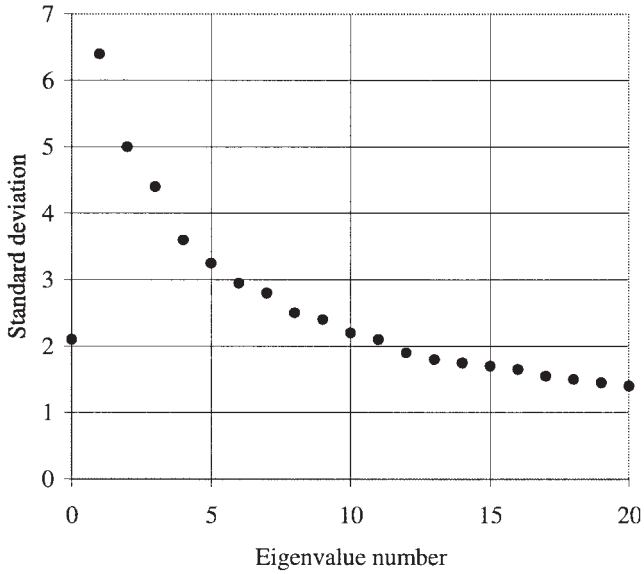

Figure 4. Standard deviation a^i_{rms} for the first 20 eigenfunctions.

When projecting instantaneous velocity fields on eigenfunctions obtained from POD one obtains

$$a_k^i = (\mathbf{\Phi}_i, U_k) \tag{8}$$

Or for a given phase θ (with conditioned velocity fields):

$$a_k^{i,\theta} = (\mathbf{\Phi}_i, U_k^\theta) \tag{9}$$

It is then possible to compute a global averaged value $\overline{a_k^i}$ associated with the corresponding rms deviation a^i_{rms}, and phased averaged values of this projections $\langle a_k^{i,\theta}\rangle_\theta$ with the rms deviation $a^{i,\theta}_{rms}$ for a given phase θ.

As illustrated by the curve in Figure 4, the rms value a^i_{rms} reaches a maximum after projecting on mode 1 and 2. This means that the coherent structures associated with these modes, weighted by the reconstruction coefficient, undergoes large spatial variations between all phase velocity fields. The main difference between velocity fields from different blade positions consists in trailing vortex position. Indeed, the trajectory of the vortices has been shown to follow the phase-averaged velocity fields induced by the impeller (Escudié and Liné[9]). Then it is possible that mode 1 and 2 are linked with these vortices. Figure 5 shows $a^{i,\theta}_{rms}$ for different value of θ. For each value of θ the largest value of $a^{i,\theta}_{rms}$ is after projecting in mode 3. Then this mode carries the main structural difference between velocity fields from phase θ. One way to analyse POD modes contribution is to compose a velocity field with an admixture of modes (Patte-Rouland et al.[13])

$$U = \langle a_0\rangle\mathbf{\Phi}_0 + \sum_i (\langle a_i\rangle \pm \sigma_i)\mathbf{\Phi}_i \tag{10}$$

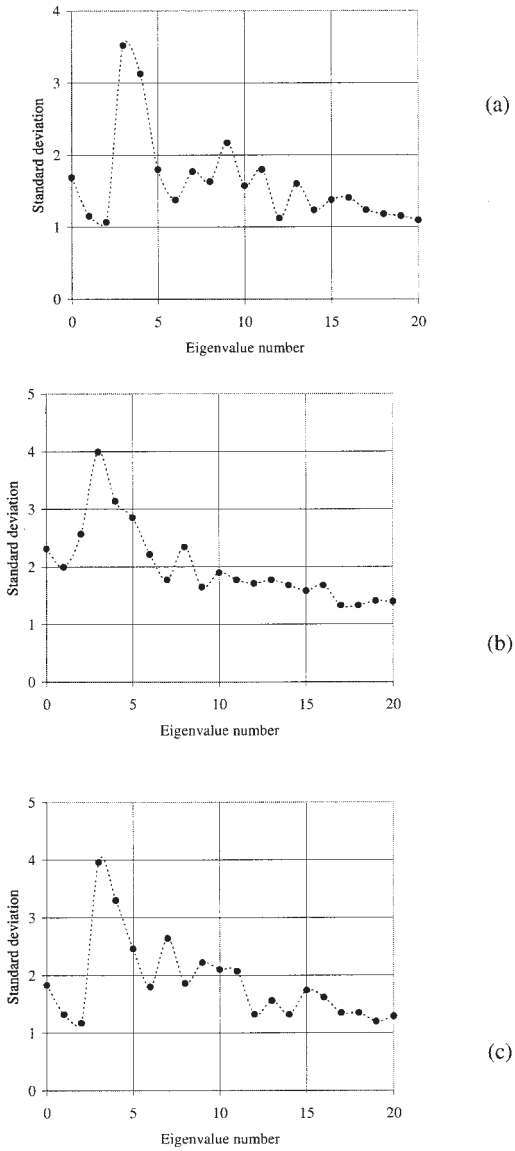

Figure 5. Standard deviation $a^{i,\theta}_{rms}$ for the first 20 eigenfunctions for different blade positions (a) θ = 5°, (b) θ = 30°, (c) θ = 55°.

where σ_i is the mean projection variance.

The reconstruction of one velocity field using mode 0 and mode 3 with $a^0 = 160$, and three values of a^3 namely 60, 0 and -60, is represented in Figure 6. It shows the influence of the value of a^3 on the structure of the flow, and especially on the jet flapping, the horizontal jet having periodic fluctuations in terms of vertical displacements above and below the mean position. The main difference between two fields of a given phase consists in the jet position thus leading to the conclusion that mode 3 is linked with jet flapping.

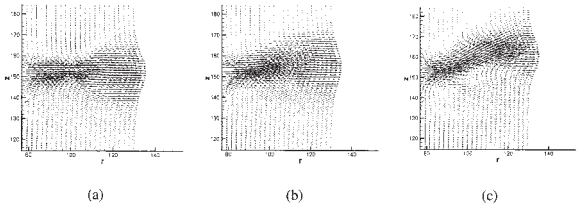

Figure 6. Reconstruction simulations of a velocity field with a^0 = 160, and severals values of a^3 = −60 (a), a^3 = 0 (a) and a^3 = 60 (a).

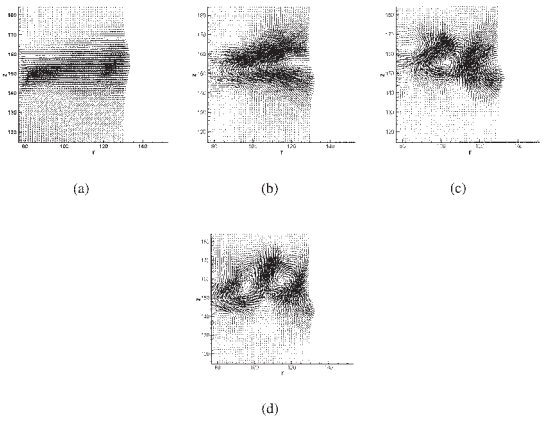

Figure 7. (a) Mode 0, (b) mode 1, (c) mode 2, (d) mode 3, from POD of the all set of velocity fields without periodic fluctuations contribution.

POD applied to instantaneous velocity fields, synchronized with blade position, substracting periodic fluctuations

In order to confirm the link between mode 1, 2 and the trailing vortices, we decided to carried out a second POD decomposition procedure using velocity field U^* without periodic fluctuation following the systematic operation

$$U^* = U - \tilde{u} \tag{11}$$

This decomposition leads to a set of eigenfunctions $\{\mathbf{\Phi}^*_i\}$, and the associated eigenvalues λ^*_i. Figure 7 shows the mode 0, 1, 2 and 3 (respectively, $\mathbf{\Phi}^*_0$, $\mathbf{\Phi}^*_1$, $\mathbf{\Phi}^*_2$ and $\mathbf{\Phi}^*_3$) of this decomposition. The main result is that the structure of $\mathbf{\Phi}^*_1$ corresponds to $\mathbf{\Phi}_3$. This is a very important result since it signifies that the second POD procedure does not lead to modes $\mathbf{\Phi}_1$ and $\mathbf{\Phi}_2$. Then it confirms that these modes are linked with the periodic fluctuations.

It is then possible to determine the fluctuating kinetic energy $\tilde{E}c = \overline{(\tilde{u} + \tilde{v})}$ of the periodic motion by calculating statistics of velocity fields reconstructed with modes 0, 1 and 2 and corresponding projection coefficients. It is interesting to note that in Figure 8 the integrated kinetic energy calculated from the original velocity fields has a good agreement with the integrated kinetic energy obtained with the reconstructed fields with modes 0-1-2. The plot of the fluctuating energy for fields reconstructed with modes 0-1 shows that this low order model is not sufficient to rebuilt the dynamics of the periodic structures. In addition to this one can note that the order of the reconstruction with modes 0-1-2-3 is high, such as the fluctuating energy must contains flapping jet and smaller scales energy. Modes 1 and 2 seems definitely linked with the trailing vortices.

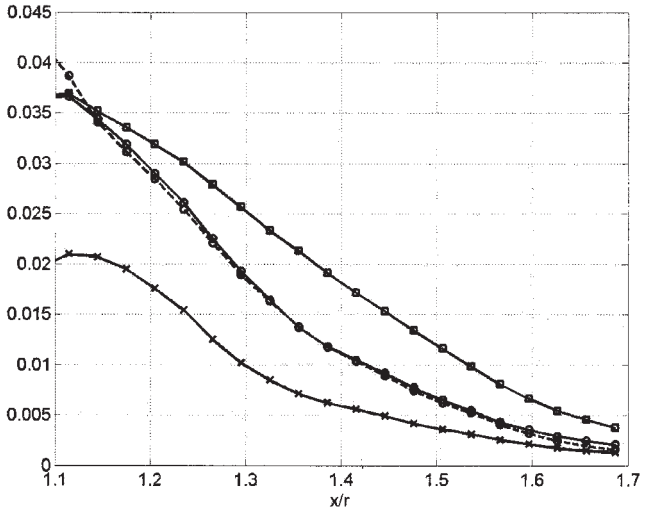

Figure 8. Mean kinetic periodic energy $\tilde{E}t$ x-profile for different recontructed fields, and for original fields: 'x' velocity fields recontructed with mode 0 and mode 1; '- -○' velocity fields recontructed with mode 0, 1 and mode 2; '□' velocity field recontructed with mode 0, mode 1, 2 and 3; '○' original velocity fields.

Concluding Remarks

In this article, we show that proper orthogonal decomposition associated with particle image velocimetry can be an efficient way to separate the periodic fluctuations from the turbulent fluctuations. The main result is that the POD decomposition leads to characteristic modes that can be pointed out to be linked with the periodic motion of the turbulent flow measured in a Rushton turbine at a fixed Reynolds number. This work is a first step in the study of energy transfer between large eddies and turbulence in the case of a Rushton turbine impeller flow. For example, it is now possible to reconstruct instantaneous velocity fields with an admixture of the first three POD modes from the decomposition of a nonphased set of fields. Then, these new fields could be compared to phase averaged fields in a view to get quantitative data concerning energy carried by the periodic flow. In this case, it would signify that one would be able to get data concerning the periodic flow without the necessity of phased measurements. Once these modes are isolated, the next step will be to produce a dynamical low-order model in order to get the best understanding of the dynamical behavior of such convective structure.

Acknowledgment

Authors would like to thank Pr. J. Borée and Pr. H.C. Boisson for their important comments about this work. Their assistance is gratefully acknowledged. The data was provided during R. Escudié Ph-D works (Escudié[14]).

Literature Cited

1. Van't Riet K, Smith JM. The trailing vortices system produced by Rushton turbine agitators. *Chem Eng Sci.* 1975;30:1093–1105.
2. Van't Riet K, Bruijn W, Smith JM. Real and pseudo turbulence in the discharge stream from a rushton turbine. *Chem Eng Sci.* 1976;31:407–412.
3. Escudié R, Bouyer D, Liné A. Experimental analysis of trailing vortices in radially agitated tank. *AIChE J.* 2004;50:75–86.
4. Wu H, Patterson GK. Laser Doppler measurements of turbulent flow parameters of a stirred mixer. *Chem Eng Sci.* 1989;44:2207–2221.
5. Yianneskis M, Whitelaw JH. On the structure of trailing vortices around a Rushton turbine blades. *Trans Inst Chem Eng.* 1993;71:543–550.
6. Stoots C, Calabrese RV. Mean velocity field relative to a Rushton turbine blade. *AIChE J.* 1995;41:1–11.
7. Schäfer M, Yu J, Geneger B, Durst F. Turbulence generation by different types of implellers. Proc. 10th European Conference on Mixing. Delft, Netherlands. 2000:9–16.
8. Sharp KV, Adrian RJ. PIV study of small-scale flow structure around a Rushton turbine. *AIChE J.* 2001;47:766–778.
9. Escudié R, Liné A. Experimental analysis of hydrodynamics in a radially agitated tank. *AIChE J.* 2003;49:585–603.
10. Reynolds WC, Hussain AKMF. The mechanics of an organized wave in turbulent shear flow. Part 3. Theoretical models and comparisons with experiments. *J Fluid Mech.* 1972;54:263–288.
11. Lumley JL. *The structure of inhomogeneous turbulence.* In: Yaglom AM and Tatarski VI, eds. Nauka: Moscow; 1967;166–178.
12. Sirovich L. Turbulence and the dynamics of coherent structures. Part 1: Coherent structures. *Quarterly of Applied Mathematics.* 1987;45:561–571.
13. Patte-Rouland B, Lalizel G, Moreau J, Rouland E. Flow analysis of an annular jet by particle image velocimetry and proper orthogonal decomposition. *Meas Sci Technol.* 2005;12:1404–1412.
14. Escudié R. *Structure locale de l'hydrodynamique générée par une turbine de Rushton.* Ph-D report, n°628, INSA de Toulouse: France; 2001.

Manuscript received Apr. 13, 2005, revision received Oct. 6, 2005, and final revision received Mar. 6, 2006.